

Synthesis, Characterization, Optical Properties and Theoretical Studies of Novel Substituted Imidazo[1,5-*a*]pyridinyl 1,3,4-Oxadiazole Derivatives

Yan-Qing Ge · Teng Wang · Gui Yun Duan ·
Li Hua Dong · Xiao Qun Cao · Jian Wu Wang

Received: 26 March 2012 / Accepted: 20 June 2012
© Springer Science+Business Media, LLC 2012

Abstract Novel imidazo[1,5-*a*]pyridinyl 1,3,4-Oxadiazole derivatives were synthesized and characterised by IR, ¹H NMR and HRMS. UV-vis absorption and fluorescence properties of these compounds in different solutions showed that the maximal emission wavelength was not significantly changed in different solvents; however, maximum absorption wavelength was blue-shifted with the increase of solvent polarity. Absorption λ_{max} and emission λ_{max} was less correlated with substituent groups on benzene rings. The calculated molecular orbital correlates well with their absorption.

Keywords Synthesis · Oxadiazole · Imidazo[1,5-*a*]pyridine · Nitrogen-bridgehead · UV-vis absorption · Fluorescence

Introduction

Imidazo[1,5-*a*]pyridine derivatives have been of particular interest for their pharmacological and biological activities such as cardiogenic agents [1], aromatase inhibitors in estrogen-dependent diseases [2], thromboxane A2 synthetase inhibitors [3] and angiotensin II receptor antagonists [4]. They also have potential applications in organic light-emitting diodes (OLEDs) [5–7], in organic thin-layer field

effect transistors (FETs) [8] and as precursors of N-heterocyclic carbenes [9].

Aromatic 1, 3, 4-oxadiazole-based compounds have attracted intense attention for their potential use in organic electronics because either polymers or small molecules of this kind have been widely used as electron-transporting materials or electroluminescence (EL) materials in organic light emitting diodes (OLEDs) [10–20]. In addition, electron-transporting 1, 3, 4-oxadiazole moiety has been connected to many chelating ligands to obtain luminescent complexes with more new functions [21–24].

We are interested in design, synthesis, structural characterization and fluorescence properties of novel compounds with potential bioactivity. In our previous work we reported a series of novel 2, 5-disubstituted 1, 3, 4-oxadiazole derivatives and investigated their optical properties [25]. In continuation of our efforts in synthesizing various bioactive molecules [26–30] and fluorescent small molecules [31–33], herein, we report the synthesis, characterization and optical properties of novel 1, 3, 4-oxadiazole derivatives combined with imidazo[1,5-*a*]pyridine in order to investigate their potential application in localization of small molecule in cells.

Experimental

General

Thin-layer chromatography (TLC) was conducted on silica gel 60 F₂₅₄ plates (Merck KGaA). ¹H NMR spectra were recorded on a Bruker Avance 400 (400 MHz) spectrometer, using DMSO-*d*₆ as solvent and tetramethylsilane (TMS) as internal standard. Melting points were determined on an XD-4 digital micro melting point apparatus. IR spectra were recorded with an IR spectrophotometer VERTEX 70 FT-IR (Bruker Optics). The High Resolution Mass Spectrometry

Y.-Q. Ge · T. Wang · G. Y. Duan · L. H. Dong · X. Q. Cao (✉)
Taishan Medical University,
Taian, Shandong 271016, People's Republic of China
e-mail: xqcao@yahoo.cn

J. W. Wang (✉)
School of Chemistry and Chemical Engineering,
Shandong University,
Jinan, Shandong 250100, People's Republic of China
e-mail: jwwang@sdu.edu.cn

(HRMS) spectra were recorded on a Q-TOF6510 spectrophotometer (Agilent). UV-vis spectra were recorded on a U-4100 (Hitachi). Fluorescent measurements were recorded on a Perkin-Elmer LS-55 luminescence spectrophotometer.

Computation Details

The hybrid density function B3LYP (Becke-Lee-Young-Parr composite of exchange-correction functional) method [34, 35] and the standard 6-31G (d, p) basis set [36] were used for both structure optimization and the property calculations. All the calculations were performed using the Gaussian 03 program in the IBM P690 system at the Shandong Province High Performance Computing Centre.

General Procedure for Preparation of 2-(3-butyl-1-chloroimidazo[1,5-a]pyridin-7-yl)-5-(chloromethyl)-1,3,4-oxadiazole 3

To a solution of 3-butyl-1-chloroimidazo[1,5-a]pyridine-7-carbohydrazide (**1**) (3.5 mmol) in dichloromethane (50 ml) was added 15 drops of Et₃N. Subsequently, the solution of 2-chloroacetyl chloride (4.2 mmol) dissolved in dichloromethane (5 ml) was added dropwise in 20 min at room temperature. The reaction mixture was stirred for 6 h at room temperature, after which the solvent was removed under reduced pressure. Water (30 ml) was added to the residue to remove soluble impurity and the precipitate was filtrated, washed with water (10 ml×3) and dried to give **2** without further purification. The mixture of **2** (3.5 mmol) and POCl₃ (15 ml) was refluxed for 8 h. After cooling, it was poured into powder ice (100 g). The precipitate was filtrated, washed with water and dried. Product **3** was obtained by column chromatography on silica gel using PE/EtOAc (4:1) as an eluent.

General Procedure for Preparation of 2-(3-butyl-1-chloroimidazo[1,5-a]pyridin-7-yl)-5-(aryloxymethyl)-1,3,4-oxadiazole 5a-i

A mixture of **3** (1 mmol), substituted phenol **4** (1.05 mmol), anhydrous potassium carbonate (1.2 mmol) and dry acetonitrile (25 ml) was refluxed for 1–3 h, after which the solution was condensed under reduced pressure. The residue was extracted with dichloromethane (30 ml). The organic phase was washed with 5 % NaOH solution (10 ml), water (10 ml×3) and dried over MgSO₄. After filtered, the filtrate was concentrated under reduced pressure to afford title compound **5** in 82–92 % (Fig. 1).

The Spectroscopic Data of Compounds 5

2-(3-butyl-1-chloroimidazo[1,5-a]pyridin-7-yl)-5-(phenoxy-methyl)-1,3,4-oxadiazole (5a) Yellow solid (90 % yield):

mp 130.6–130.9 °C; ¹H NMR (400 MHz, DMSO-*d*₆): δ 8.40 (d, *J*=7.2 Hz, 1H), 7.98 (s, 1H), 7.35 (m, 2H), 7.18 (dd, *J*=7.6, 1.6 Hz, 1H), 7.12 (d, *J*=8.0 Hz, 2H), 7.03 (m, 1H), 5.49 (s, 2H), 3.02 (t, *J*=7.2 Hz, 2H), 1.73 (m, 2 H), 1.38 (m, 2H), 0.92 (t, *J*=7.2 Hz, 3H); IR (KBr) ν=2945, 2872, 1638, 1601, 1494, 1403, 1220, 1078, 749 cm⁻¹; HRMS: *m/z* calcd for C₂₀H₂₀ClN₄O₂ [M+H]⁺ 383.1275, found 383.1288.

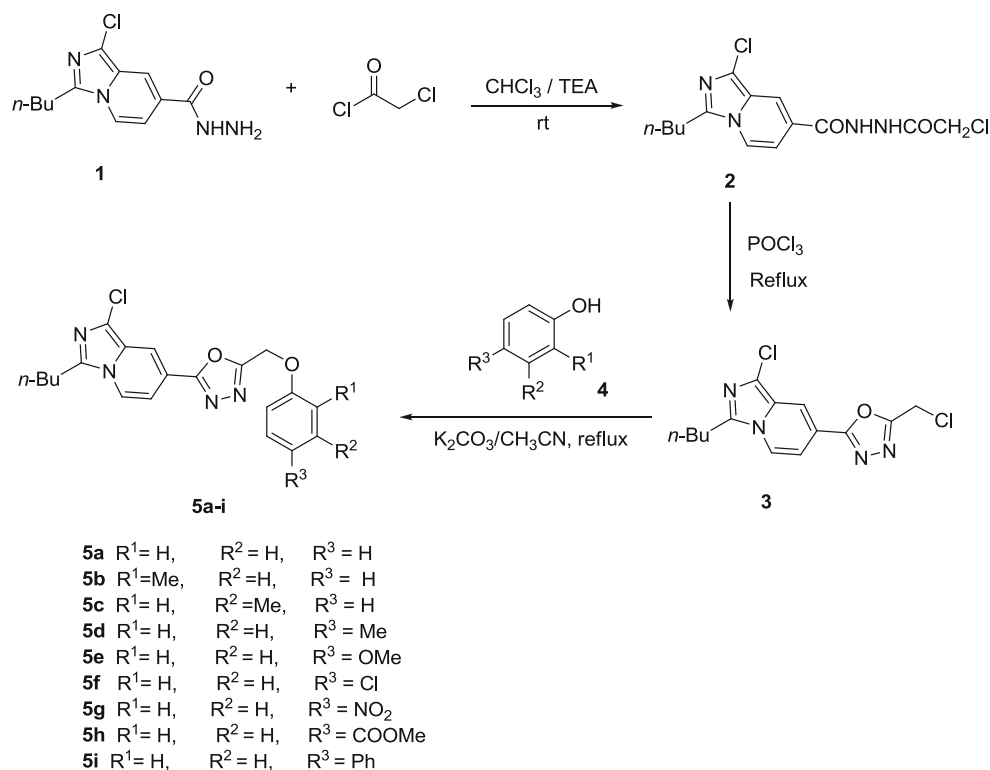
2-(3-butyl-1-chloroimidazo[1,5-a]pyridin-7-yl)-5-(*o*-toloxymethyl)-1,3,4-oxadiazole (5b) Yellow solid (86 % yield): mp 127.7–128 °C; ¹H NMR (400 MHz, DMSO-*d*₆): δ 8.41 (dd, *J*=7.6, 0.8 Hz, 1H), 7.98 (s, 1H), 7.22–7.16 (m, 4H), 6.94 (m, 1H), 5.50 (s, 2H), 3.02 (t, *J*=7.2 Hz, 2H), 2.21 (s, 3H), 1.73 (m, 2 H), 1.38 (m, 2H), 0.92 (t, *J*=7.2 Hz, 3H); IR (KBr) ν=2954, 2868, 1637, 1591, 1494, 1289, 1251, 1128, 1078, 748 cm⁻¹; HRMS: *m/z* calcd for C₂₁H₂₂ClN₄O₂ [M+H]⁺ 397.1431, found 397.1426.

2-(3-butyl-1-chloroimidazo[1,5-a]pyridin-7-yl)-5-(*m*-toloxymethyl)-1,3,4-oxadiazole (5c) Yellow solid (92 % yield): mp 126.1–126.9 °C; ¹H NMR (400 MHz, DMSO-*d*₆): δ 8.39 (d, *J*=7.2 Hz, 1H), 7.96 (s, 1H), 7.24–7.16 (m, 2H), 6.90–6.95 (m, 2H), 6.84 (d, *J*=7.2 Hz, 1H), 5.46 (s, 2H), 3.02 (t, *J*=7.2 Hz, 2H), 2.30 (s, 3H), 1.73 (m, 2H), 1.38 (m, 2H), 0.92 (t, *J*=7.2 Hz, 3H); IR (KBr) ν=2953, 2929, 2868, 1637, 1588, 1491, 1450, 1246, 1159, 1078, 769 cm⁻¹; HRMS: *m/z* calcd for C₂₁H₂₂ClN₄O₂ [M+H]⁺ 397.1431, found 397.1424.

2-(3-butyl-1-chloroimidazo[1,5-a]pyridin-7-yl)-5-(*p*-toloxymethyl)-1,3,4-oxadiazole (5d) Yellow solid (88 % yield): mp 154.4–154.9 °C; ¹H NMR (400 MHz, DMSO-*d*₆): δ 8.39 (dd, *J*=7.6, 0.8 Hz, 1H), 7.97 (d, *J*=0.8 Hz, 1H), 7.18–7.13 (m, 3H), 7.00 (d, *J*=8.8 Hz, 2H), 5.43 (s, 2H), 3.02 (t, *J*=7.2 Hz, 2H), 2.25 (s, 3H), 1.73 (m, 2H), 1.38 (m, 2H), 0.92 (t, *J*=7.2 Hz, 3H); IR (KBr) ν=2966, 2869, 1711, 1638, 1589, 1481, 1456, 1277, 1031, 752 cm⁻¹; HRMS: *m/z* calcd for C₂₁H₂₂ClN₄O₂ [M+H]⁺ 397.1431, found 397.1431.

2-(3-butyl-1-chloroimidazo[1,5-a]pyridin-7-yl)-5-((4-methoxyphenoxy)methyl)-1,3,4-oxadiazole (5e) Yellow solid (82 % yield): mp 128.8–129.8 °C; ¹H NMR (400 MHz, DMSO-*d*₆): δ 8.39 (d, *J*=7.6 Hz, 1H), 7.97 (s, 1H), 7.17 (d, *J*=7.6 Hz, 1H), 7.06 (d, *J*=8.8 Hz, 2H), 6.90 (d, *J*=8.8 Hz, 2H), 5.41 (s, 2H), 3.71 (s, 3H), 3.02 (t, *J*=7.2 Hz, 2H), 1.73 (m, 2H), 1.38 (m, 2H), 0.92 (t, *J*=7.2 Hz, 3H); IR (KBr) ν=2958, 2933, 2872, 1635, 1580, 1564, 1508, 1494, 1403, 1231, 1044, 813, 727 cm⁻¹; HRMS: *m/z* calcd for C₂₁H₂₂ClN₄O₃ [M+H]⁺ 413.1830, found 413.1842.

2-(3-butyl-1-chloroimidazo[1,5-a]pyridin-7-yl)-5-((4-chlorophenoxy)methyl)-1,3,4-oxadiazole (5f) Yellow solid (87 %

Fig. 1 The synthetic route of unsymmetrical 1,3,4-oxadiazole derivatives

yield): mp 155.9–156.7 °C; ¹H NMR (400 MHz, DMSO-*d*₆): δ 8.39 (d, *J*=7.6 Hz, 1H), 7.97 (s, 1H), 7.39 (d, *J*=8.8 Hz, 2H), 7.18–7.15 (m, 3H), 5.51 (s, 2H), 3.02 (t, *J*=7.2 Hz, 2H), 1.73 (m, 2H), 1.38 (m, 2H), 0.92 (t, *J*=7.2 Hz, 3H); IR (KBr) ν =2958, 2929, 2864, 1638, 1585, 1560, 1493, 1226, 1078, 819, 722 cm⁻¹; HRMS: *m/z* calcd for C₂₀H₁₉Cl₂N₄O₂ [M+H]⁺ 417.0885, found 417.0891.

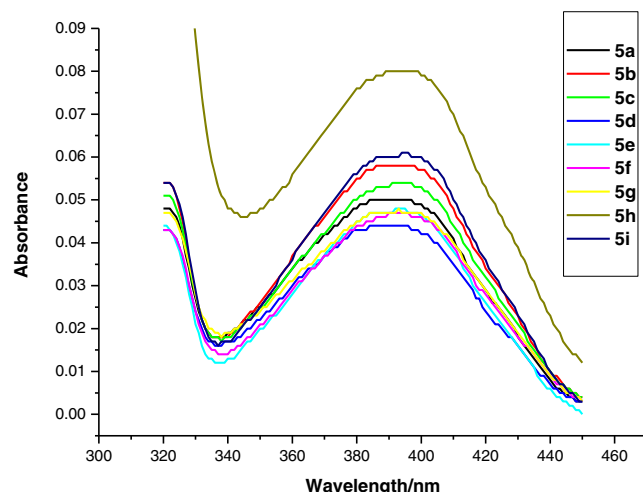
2-(3-butyl-1-chloroimidazo[1,5-*a*]pyridin-7-yl)-5-((4-nitrophenoxy)methyl)-1,3,4-oxadiazole (**5g**) Yellow solid (85 % yield): mp 166–167.3 °C; ¹H NMR (400 MHz, DMSO-*d*₆): δ 8.39 (d, *J*=7.6 Hz, 1H), 8.29–8.25 (m, 2H), 7.98 (s, 1H),

7.38–7.34 (m, 2H), 7.17 (dd, *J*=7.6, 1.6 Hz, 1H), 5.70 (s, 2H), 3.02 (t, *J*=7.2 Hz, 2H), 1.73 (m, 2H), 1.38 (m, 2H), 0.92 (t, *J*=7.2 Hz, 3H); IR (KBr) ν =2962, 2929, 2864, 1637, 1593, 1513, 1494, 1343, 1299, 1074, 747 cm⁻¹; HRMS: *m/z* calcd for C₂₀H₁₉ClN₅O₄ [M+H]⁺ 428.1126, found 428.1133.

Methyl 4-((5-(3-butyl-1-chloroimidazo[1,5-*a*]pyridin-7-yl)-1,3,4-oxadiazol-2-yl)methoxy)benzoate (**5h**) Yellow solid (90 % yield): mp 155.9–157 °C; ¹H NMR (400 MHz, DMSO-*d*₆): δ 8.39 (d, *J*=7.6 Hz, 1H), 7.97 (s, 1H), 7.95

Table 1 Maximum absorption wavelength (λ_{\max}) and maximum molar extinction coefficients (ϵ_{\max}) of **5a-i** in dichloromethane and acetonitrile

Compound	λ_{\max}		E (mol ⁻¹ cm ⁻¹ L)	
	CH ₃ CN	DCM	CH ₃ CN	DCM
5a	377	390	32000	50000
5b	377	392	37000	58000
5c	378	394	33000	54000
5d	361	390	29000	44000
5e	375	393	32000	48000
5f	369	393	35000	47000
5g	368	393	27000	48000
5h	386	394	67000	80000
5i	367	395	53000	61000

**Fig. 2** UV-vis absorption spectra of **5a-i** in dichloromethane solution (10⁻⁶ M)

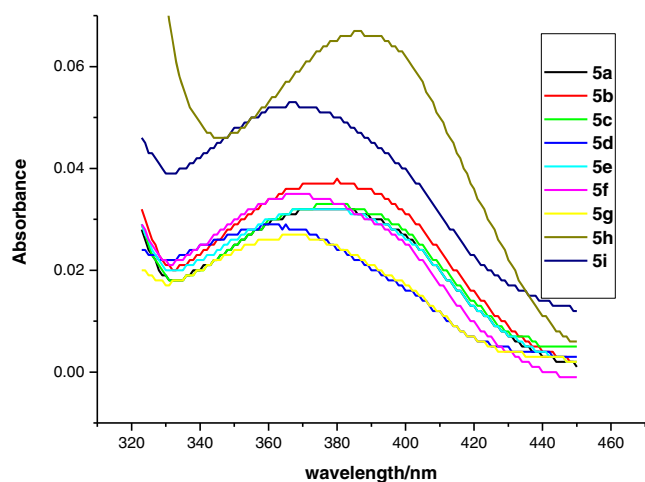


Fig. 3 UV-vis absorption spectra of **5a-i** in acetonitrile solution (10^{-6} M)

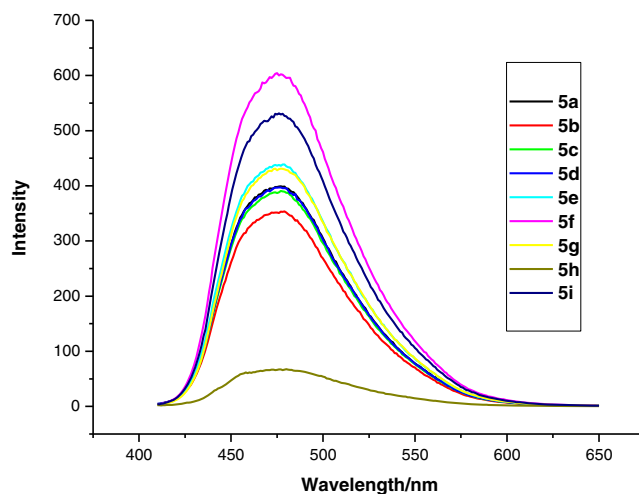


Fig. 5 Fluorescence spectra of the compounds **5a-i** in acetonitrile (10^{-6} M)

(d, $J=9.2$ Hz, 2H), 7.24 (d, $J=8.8$ Hz, 2H), 7.17 (dd, $J=7.6$, 1.6 Hz, 1H), 5.61 (s, 2H), 3.83 (s, 3H), 3.02 (t, $J=7.2$ Hz, 2H), 1.73 (m, 2H), 1.38 (m, 2H), 0.92 (t, $J=7.2$ Hz, 3H); IR (KBr) $\nu=2956$, 2875, 1720, 1636, 1607, 1510, 1493, 1282, 1170, 1040, 767 cm^{-1} ; HRMS: m/z calcd for $\text{C}_{22}\text{H}_{22}\text{ClN}_4\text{O}_4$ $[\text{M}+\text{H}]^+$ 441.1330, found 441.1319.

2-((biphenyl-4-yloxy)methyl)-5-(3-butyl-1-chloroimidazo[1,5-a]pyridin-7-yl)-1,3,4-oxadiazole (5i) Yellow solid (88 % yield); mp 145.9–146.5 $^{\circ}\text{C}$; ^1H NMR (400 MHz, $\text{DMSO}-d_6$): δ 8.39 (d, $J=7.6$ Hz, 1H), 7.84 (s, 1H), 7.54 (d, $J=7.6$ Hz, 1H), 7.43–7.29 (m, 6H), 7.16–7.11 (m, 2H), 5.50 (s, 2H), 3.02 (t, $J=7.2$ Hz, 2H), 1.73 (m, 2H), 1.38 (m, 2H), 0.92 (t, $J=7.2$ Hz, 3H); IR (KBr) $\nu=2933$, 2870, 1633, 1584, 1559, 1508, 1492, 1206, 1073, 810, 723 cm^{-1} ; HRMS: m/z calcd for $\text{C}_{26}\text{H}_{24}\text{ClN}_4\text{O}_2$ $[\text{M}+\text{H}]^+$ 459.1588, found 459.1586.

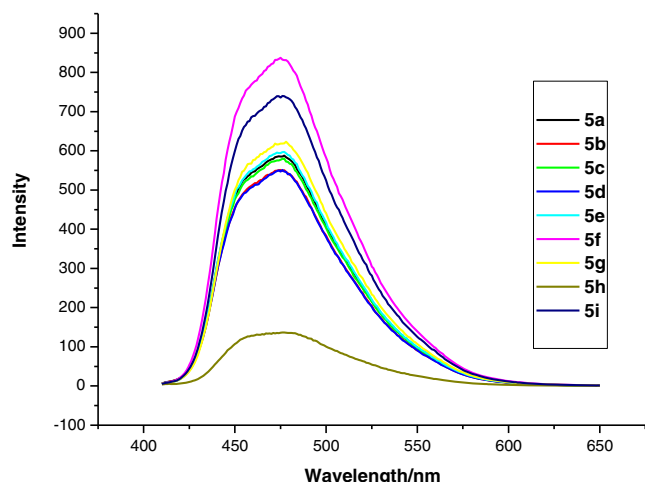


Fig. 4 Fluorescence spectra of compounds **5a-i** in dichloromethane (10^{-6} M)

Results and Discussion

Synthesis and Characterization

The synthetic procedures of compound **5a-i** are shown in Fig. 1. The starting 3-butyl-1-chloroimidazo[1,5-a]pyridine-7-carbohydrazide **1** can be easily prepared according to the procedure reported in our previous paper [25]. The reaction of **1** and 2-chloroacetyl chloride in the presence of triethylamine in dichloromethane at room temperature afforded intermediate **2** that can be used to the next reaction step without further purification. Then **2** reacted with phosphoryl trichloride to give 2-(3-butyl-1-chloroimidazo[1,5-a]pyridin-7-yl)-5-(chloromethyl)-1,3,4-oxadiazole **3** that can be purified by column chromatography on silica gel using PE/EtOAc (4:1) as an eluent. The reaction of **3** and substituted phenol **4** in the presence of anhydrous potassium

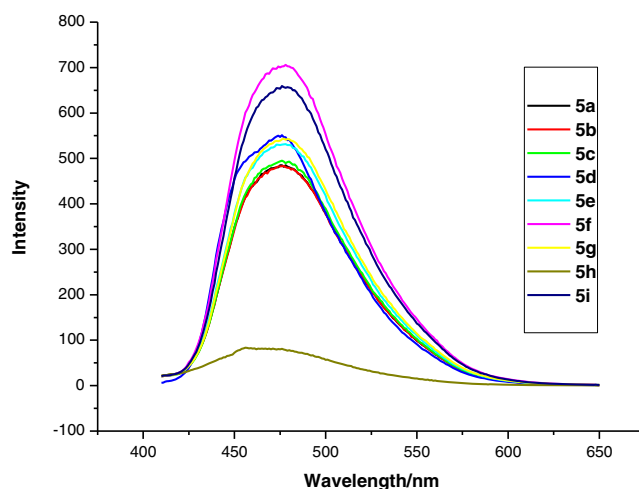


Fig. 6 Fluorescence spectra of the compounds **5a-i** in DMF (10^{-6} M)

Table 2 Maximum wavelength of excitement and emission of fluorescence of compounds **5a-i**

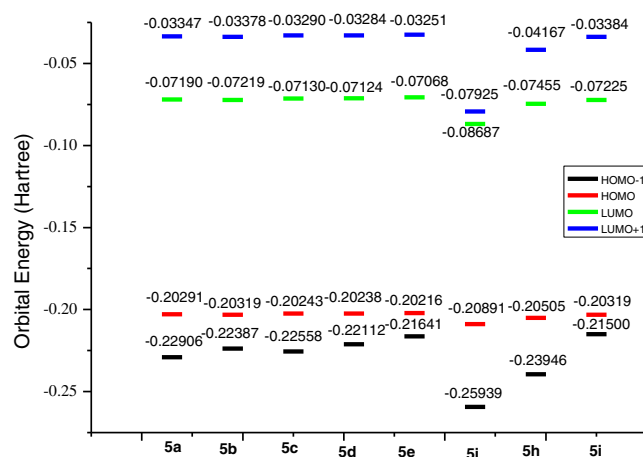
Compound	λ_{ex} (nm)	λ_{em} (nm)		
		DCM	CH ₃ CN	DMF
5a	390	477	477	476
5b	390	475	479	477
5c	390	477	477	476
5d	390	476	476	476
5e	390	477	479	478
5f	390	475	475	478
5g	390	478	474	477
5h	390	476	476	476
5i	390	476	474	476

carbonate in dry acetonitrile at reflux temperature afforded compound **5** in 82–92 %.

The proposed structures were confirmed by ¹H NMR spectra, IR, and HRMS.

Absorption Spectra of the Compounds **5a-i**

For UV-visible absorption measurements, the concentration was 5×10^{-6} mol L⁻¹, and the absorption data are summarized in Table 1. The UV-visible absorption spectra of compounds **5a-i** measured in dichloromethane and acetonitrile solutions are given in Figs. 2 and 3. These compounds displayed similar absorptions ranging from 367 to 394 nm that were attributed to π - π transition of conjugation system. Comparing with 2-(3-butyl-1-chloroimidazo[1,5-a]pyridin-7-yl)-5-aryl-1,3,4-oxadiazole reported in previous paper [25], compounds **5a-i** have blue shifted about 20 nm, the reason being that the aryloxy which are linked to methylene in C5 cannot extend to the pi-conjugation system due to the block effect of methylene. It is also observed that the λ_{max} values of **5a-i** change with the polarity of solutions. Generally in different solvents, there is a consequence for the λ_{max}

**Fig. 8** Molecular orbital energy levels of compounds **5a-i**

values of **5a-i**: λ_{max} (DCM) > λ_{max} (CH₃CN). In the same solvent compounds **5a-i** have the similar maximum absorption, which means substituent R¹, R² and R³ have no significant impact on the absorption. The maximum molar extinction coefficients of **5a-i** in dichloromethane and acetonitrile are different, and it can be observed that the enhancement order is generally ϵ (CH₃CN) < ϵ (DCM).

Fluorescence Spectra

The emission spectra of compounds **5a-i** in dichloromethane, acetonitrile and DMF solution (10^{-6} mol L⁻¹) are presented in Figs. 4, 5 and 6 respectively and their excitation wavelengths are shown in Table 2. It can be found that their intensity of fluorescence differed from each other. In comparison with the effect on the absorption spectrum, the group in benzene ring had weak influence on the emission intensity of 1,3,4-oxadiazole compounds except compound **5h** with a methoxycarbonyl group. It can be seen from Table 2 that the maximum emission wavelengths of **5a-i** are almost the same in three solvents. These results indicate that the environment plays no significant role in determining

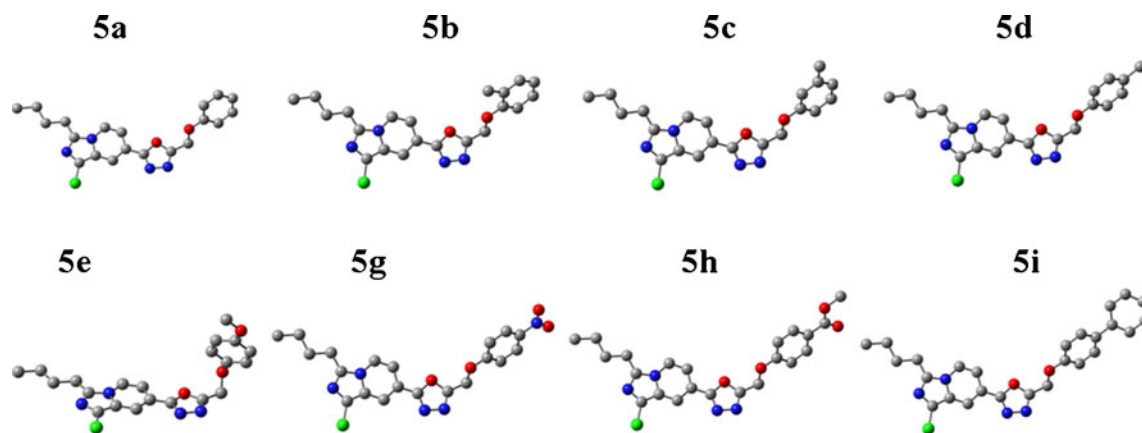
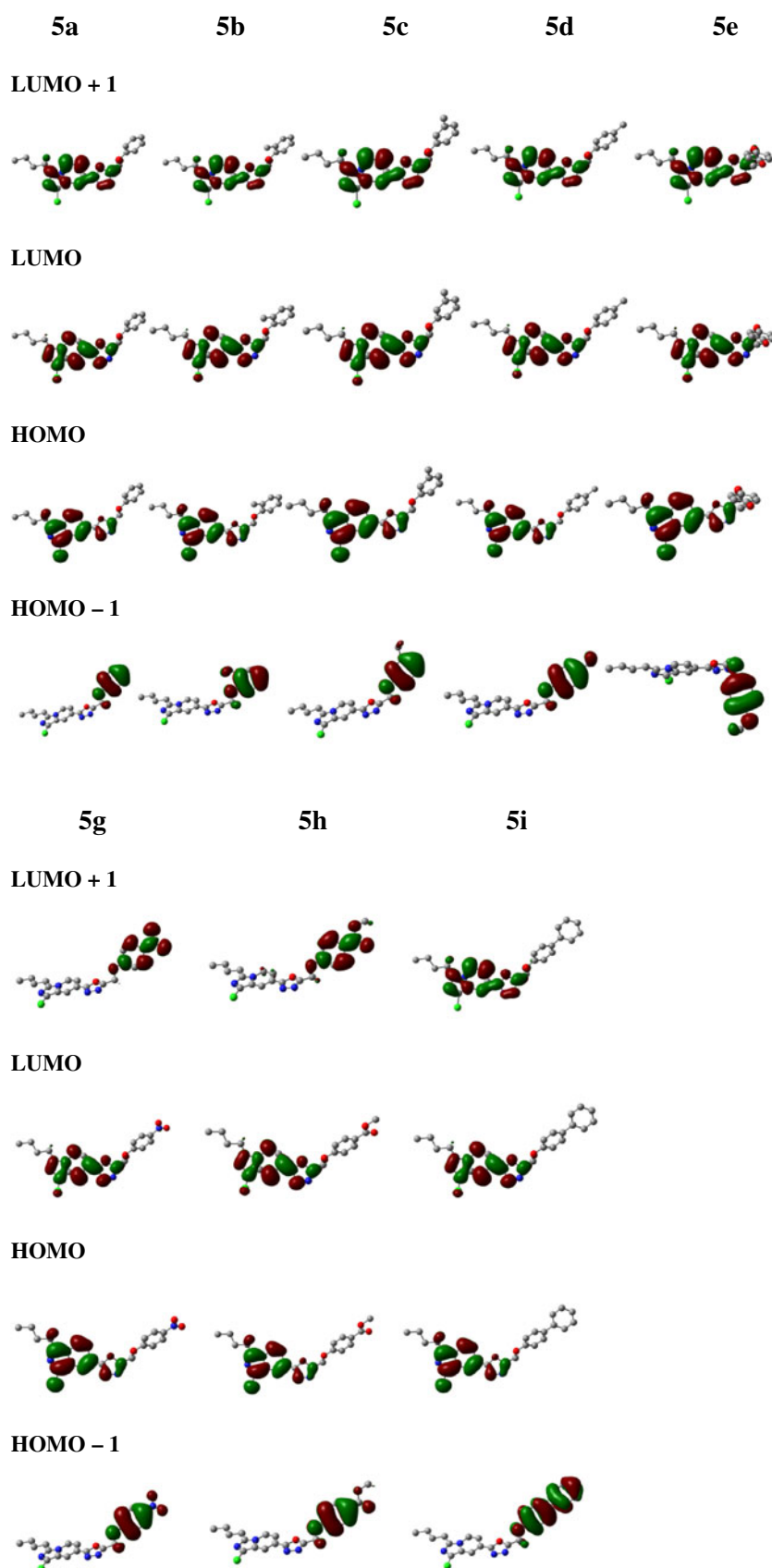
**Fig. 7** The minimized structures of compounds **5**

Fig. 9 Molecular orbital maps of compounds **5**



the emission wavelengths of the compounds. However, the fluorescence intensity decreased with the increase in solvent polarity. It is believed that the potential energy surface of the emitting state is different from that of the ground state and a photo-induced intramolecular charge transfer (ICT) takes place in the fluorescence states with increasing solvent polarity. That is to say, the molecule is solvated significantly in the S_1 excited state, resulting in a difference in dipole moment between the S_1 excited state and the ground state.

Theoretical Calculations

To enhance our understanding of the relationship between molecular structures and the electronic spectra of these new 1,3,4-oxadiazoles derivatives, we carried out structure optimization and molecular orbital (MO) calculations on compound **5a-i** based on a simplified model with density functional theory (DFT) on the level of B3LYP. The minimized structures are shown in Fig. 7 and the calculated molecular orbital (HOMO and LUMO) energies are shown in Fig. 8.

The minimized structures of compound **5** revealed that imidazo[1,5-*a*]pyridine ring presents a coplanar conformation with the 1,3,4-oxadiazole ring while the benzene ring does not. This indicates that imidazo[1,5-*a*]pyridine group conjugates with the 1,3,4-oxadiazole ring efficiently through the single bond yet the benzene does not. This result is in accordance with the similar absorptions spectra of compound **5** with different substituents on the benzene ring.

The molecular energy levels of the frontier molecular orbital shown in Fig. 8 revealed that the introduction of electron-withdrawing group to benzene ring raised the energy levels of HOMO and also raised the energy levels of LUMO for the compound; therefore, the energy gap between HOMO and LUMO changed little. This corresponds well to the experimentally recorded similar absorption spectra of compound **5**.

The frontier molecular orbital maps of compound **5** in Fig. 9 revealed that the contribution of the benzene group to HOMO and LUMO is small. Therefore, the calculated results explain well the similar absorption maximum of compound **5a-i** because of the little contribution of the benzene group to HOMO and LUMO.

Conclusion

In summary, a series of novel substituted 1,3,4-oxadiazole-containing imidazo[1,5-*a*]pyridine derivatives have been synthesized. The structures of the compounds obtained were determined by IR, ^1H NMR and HRMS spectra. Studies on the optical properties indicate that the substituents on benzene ring have no significant impact on the UV-vis

absorption and fluorescence emission. Quantum calculation correlates well with their absorption and fluorescence emission. However, the maximum absorption wavelength changes significantly with the increase of solvent polarity. In contrast with the previous report, present work provides small molecules with more interesting structure diversity and similar optical properties. Currently, investigations are underway to elucidate the bioactivity and localization of small molecule in cells and the results will be reported in due course.

Acknowledgement This study was supported by the Science and Technology Development Project of Shandong Province (2011GGH22112 and 2012GSF11812).

References

1. Davey D, Erhardt PW, Lumma WC Jr, Wiggins J, Sullivan M et al (1987) Cardiotonic agents. 1. Novel 8-aryl substituted imidazo[1,2-*a*]- and -[1,5-*a*]pyridines and imidazo[1,5-*a*]pyridinones as potential positive inotropic agents. *J Med Chem* 30:1337–1342
2. Browne LJ, Gude C, Rodriguez H, Steele RE (1991) Fadrozole hydrochloride: a potent, selective, nonsteroidal inhibitor of aromatase for the treatment of estrogen-dependent disease. *J Med Chem* 34:725–736
3. Ford NF, Browne LJ, Campbell T, Gemenden C, Goldstein R, Gude C et al (1985) Imidazo[1,5-*a*]pyridines: a new class of thromboxane A2 synthetase inhibitors. *J Med Chem* 28:164–170
4. Kim D, Wang L, Hale JJ, Lynch CL, Budhu RJ, MacCoss M et al (2005) Potent 1,3,4-trisubstituted pyrrolidine CCR5 receptor antagonists: effects of fused heterocycles on antiviral activity and pharmacokinetic properties. *Bioorg Med Chem Lett* 15:2129–2134
5. Nakatsuka M, Shimamura T. JP 2001035664
6. Tominaga G, Kohama R, Takano A. JP 2001006877
7. Kitazawa D, Tominaga G, Takano, A. JP 2001057292
8. Salassa L, Garino C, Albertino A, Volpi G, Nervi C, Gobrtto R et al (2008) Computational and spectroscopic studies of new rhenium (I) complexes containing pyridylimidazo[1,5-*a*]pyridine ligands: charge transfer and dual emission by fine-tuning of excited states. *Organometallics* 27:1427–1435
9. Hiroaki N, Hiroshi Y (2005) Organic thin film transistor. WO 043630
10. Jin SH, Kim MY, Kim JY, Lee K, Gal YS (2004) *J Am Chem Soc* 126:2474–2480
11. Leung MK, Yang CC, Lee JH, Tsai HH, Lin CF, Huang CY et al (2007) *Org Lett* 9:235–238
12. Lee DW, Kwon KY, Jin JI, Park Y, Kin YR, Hwang IW (2001) *Chem Mater* 13:565–574
13. Hughes G, Bryce MR (2005) Electron-transporting materials for organic electroluminescent and electrophosphorescent devices. *J Mater Chem* 15:94–107
14. Kulkarni AP, Tonzola CJ, Babel A, Jenekhe SA (2004) *Chem Mater* 16:4556–4573
15. Kim OK, Lee KS, Woo HY, Kim KS, He GS, Swiatkiewicz J et al (2000) *Chem Mater* 12:284–286
16. Huang PH, Shen JY, Pu SC, Wen YS, Lin JT, Chou PT et al (2006) *J Mater Chem* 16:850–857
17. Qian Y, Meng K, Lu CG, Lin BP, Huang W, Cui YP (2009) *Dyes Pigments* 80:174–180
18. Goudreault T, He Z, Guo Y, Ho CL, Zhan H, Wang Q et al (2010) *Macromolecules* 43:7936–7949

19. Landis CA, Dhar BM, Lee T, Sarjeant A, Katz HE (2008) *J Phys Chem C* 112:7939–7945
20. Lee T, Landis CA, Dhar BM, Jung BJ, Sun J, Sarjeant A et al (2009) *J Am Chem Soc* 131:1692–1705
21. He Z, Wong WY, Yu XM, Kwok HS, Lin ZY (2006) Phosphorescent platinum (II) complexes derived from multifunctional multifunctional chromophores: synthesis, structures, photophysics, and electroluminescence. *Inorg Chem* 45:10922–10937
22. Chen LQ, Yang CL, Qin JG, Gao J, You H, Ma DG (2006) Synthesis, structure, electrochemistry, photophysics and electroluminescence of 1,3,4-oxadiazole-based ortho-metalated iridium(III) complexes. *J Organomet Chem* 691:3519–3530
23. Xu ZW, Li Y, Ma XM, Gao XD, Tian H (2008) Synthesis and properties of iridium complexes based 1,3,4-oxadiazoles derivatives. *Tetrahedron* 64:1860–1867
24. Li AF, Ruan YB, Jiang QQ, He WB, Jiang YB (2010) Molecular logic gates and switches based on 1,3,4-oxadiazoles triggered by metal ions. *Chem Eur J* 16:5794–5802
25. Ge YQ, Hao BQ, Duan GY, Wang JW (2011) The synthesis, characterization and optical properties of novel 1,3,4-oxadiazole-containing imidazo[1,5-a]pyridine derivatives. *J Lumin* 131(5):1070–1076
26. Ge YQ, Jia J, Li Y, Yin L, Wang JW (2009) A novel and efficient approach to pyrazolo[1,5-a]pyridine derivatives via one-pot tandem reaction. *Heterocycles* 78:197–206
27. Ge YQ, Jia J, Yang H, Zhao GL, Zhan FX, Wang JW (2009) A facile approach to indolizines via tandem reaction. *Heterocycles* 78:725–736
28. Jia J, Ge YQ, Tao XT, Wang JW (2010) Facile synthesis of imidazo[1,2-a]pyridines via tandem reaction. *Heterocycles* 81:185–194
29. Zhang DT, Jia J, Meng LJ, Xu WR, Tang LD, Wang JW (2010) Synthesis and preliminary antibacterial evaluation of 2-butyl succinate-based hydroxamate derivatives containing isoxazole rings. *Arch Pharm Res* 33(6):831–842
30. Zhang DT, Wang ZH, Xu WR, Sun FG, Tang LD, Wang JW (2009) Design, synthesis and antibacterial activity of novel actinonin derivatives containing benzimidazole heterocycles. *Eur J Med Chem* 44(5):2202–2210
31. Ge YQ, Jia J, Yang H, Tao XT, Wang JW (2011) The synthesis, characterization and optical properties of novel pyrido[1,2-a]benzimidazole derivatives. *Dyes Pigments* 88(3):344–349
32. Yang H, Mu JL, Chen X, Feng L, Jia J, Wang JW (2011) Synthesis, X-ray crystal structure and optical properties of novel 2,5-diaryl-1, 3,4-oxadiazole derivatives containing substituted pyrazolo[1,5-a]pyridine units. *Dyes Pigments* 91(3):446–453
33. Yang H, Ge YQ, Jia J, Wang JW (2011) Synthesis and optical properties of novel pyrido[1,2-a]benzimidazole-containing 1,3,4-oxadiazole derivatives. *J Lumin* 131(4):749–55
34. Becke AD (1998) Density-functional exchange-energy approximation with correct asymptotic behavior. *Phys Rev A* 38:3098–3100
35. Becke AD (1993) Density-functional thermochemistry. III. The role of exact exchange. *J Chem Phys* 98:5648–5652
36. Ong KK, Jensen JO, Hamerka HF (1999) Theoretical studies of the infrared and Raman spectra of perylene. *J Mol Struct Theochem* 459:131–144